Bioresource Technology 340 (2021) 125725

Contents lists available at ScienceDirect

Bioresource Technology

journal homepage: www.elsevier.com/locate/biortech

# Hydrothermal carbonization of distillers grains with clay minerals for enhanced adsorption of phosphate and methylene blue

Qingya Xu [a,b], Taoze Liu [a,*], Ling Li [b], Bangyu Liu [c], Xiaodan Wang [a], Shuyi Zhang [a], Liangliang Li [a], Bing Wang [d], Andrew R. Zimmerman [e], Bin Gao [f]

[a] College of Eco-Environmental Engineering, Institute of Karst Wetland Ecology, Guizhou Minzu University, Guiyang 550025, Guizhou, PR China
[b] State Key Laboratory of Environmental Geochemistry, Institute of Geochemistry, Chinese Academy of Sciences, Guiyang 550081, PR China
[c] College of Architectural Engineering, Guizhou Minzu University, Guiyang 550025, Guizhou, PR China
[d] College of Resources and Environment Engineering, Guizhou University, Guiyang 550025, Guizhou, PR China
[e] Department of Geological Sciences, University of Florida, Gainesville, FL 32611, USA
[f] Department of Agricultural and Biological Engineering, University of Florida, Gainesville, FL 32611, USA

## HIGHLIGHTS

- Novel hydrochar was prepared from distillers grains loaded with two clays.
- One-pot hydrothermal carbonization successfully synthesized the clay-hydrochar composites.
- Clay-hydrochar composites effectively adsorbed MB and P in water.
- Multiple mechanisms especially electrostatic attraction and ion exchange controlled the adsorption process.

## GRAPHICAL ABSTRACT

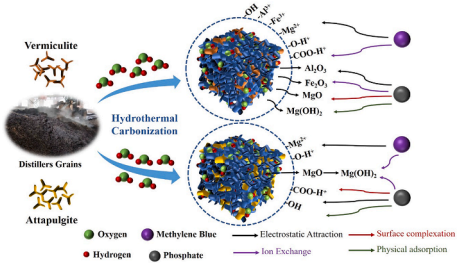


## ARTICLE INFO

*Keywords:*
Distillers grains
Modified hydrochar
Adsorption
Methylene blue
Phosphate

## ABSTRACT

A novel one-pot synthesis method was developed to prepare modified hydrochar by co-hydrothermal carbonization of waste distillers grains using low-cost clay minerals (attapulgite or vermiculite). The loading of the clay minerals onto hydrochar surfaces altered the structure and surface composition of the hydrochar such that the clay-modified hydrochars showed better ability to adsorb methylene blue and phosphate in aqueous solution than the pristine hydrochar. The maximum methylene blue and phosphate adsorption capacities of the modified hydrochar reached 340.3 and 96.9 mg $g^{-1}$, respectively, comparable or higher than that of many commercial sorbents. Multiple mechanisms, including electrostatic attraction, ion exchange, complexation, and physical adsorption, controlled the adsorption process. These results highlight excellent potential for distillers grains-derived hydrochar-clay composites as an environmental sorbent, capable of removing a variety of contaminants from aqueous solutions.

* Corresponding author.
*E-mail address:* liutaoze@foxmail.com (T. Liu).

https://doi.org/10.1016/j.biortech.2021.125725
Received 4 June 2021; Received in revised form 31 July 2021; Accepted 3 August 2021
Available online 8 August 2021

## 1. Introduction

Distillers grains are the final by-product of biomass distillation and a typical waste of the ethanol industry. Due to their high carbon and nutritional content, distillers grains are mainly used as a low-value animal feed, fertilizer, or energy source (Abd et al., 2017). Previous studies have shown that carbon-rich biomass wastes can be converted into value-added biochar products (Kumar, 2020). Nevertheless, only few studies have attempted to use distillers grains as feedstock for biochar production (Sadeghi et al., 2016; Wang et al., 2020).

Hydrothermal carbonization (HTC) is a simple, efficient, and green process for biochar (hydrochar) production (Román et al., 2020). In this process, biomass is heated uniformly in water, which enhances heat transfer and chemical reactions (Anh Tuan Vo, 2020). Because predrying of feedstock is not needed, energy consumption by hydrochar production is lower than that of biochar produced by pyrolysis (Román et al., 2020). HTC of biomass occurs in liquid water at 180–250 °C under pressures of 20–40 bar (Vinoth Kumar Ponnusamya, 2020). It involves a complex series of reactions such as dehydration, decarboxylation, decarbonylation, deamination, polymerization, condensation, and repolymerization (Miliotti et al., 2020). These reactions result in porous structures and surface functionalities that may enhance the ability of hydrochar to adsorb a range of contaminants (Zhang et al., 2018). However, the adsorption ability of most hydrochar is relatively low, especially for anions such as phosphate (Fang et al., 2015; Fang et al., 2018). Several modification technologies have been developed to improve the ability of hydrochar to sorb various pollutants in aqueous solutions (Li et al., 2020). Most of them, however, are complicated two-step methods that require HTC of the feedstock first, and then physical/chemical modification of the hydrochar. There is a crucial need to develop facile, one-pot methods that combine the HTC and modification steps to produce hydrochar with enhanced sorption ability.

Previous studies have shown the specific surface area and functional group composition of biochar to be improved through mineral modification (Wang et al., 2015; Yao et al., 2014). Minerals, especially clays, have the advantages of great abundance, low cost, large adsorption capacity, and nontoxicity (Padilla-Ortega et al., 2020; Quintelas et al., 2011). For example, Wang et al. Wang et al. (2020) found that phosphogypsum modification of biochar derived from distillers grains effectively removed phosphate (P) from water. In another study, dolomite modification greatly enhanced the removal of P from aqueous solution by biochar (Li et al., 2019). Even greater P removal, however, was achieved using Mg-containing mineral to modify biochar surfaces (Zhu et al., 2020a; Zhu et al., 2020b). These experiments indicated that the MgO particles on the surface of biochar were the main adsorption sites, and the adsorption capacity of P increased with the Mg content (Zheng et al., 2020). However, there has been no exploration of the properties and adsorption abilities of hydrochar modified with magnesium-rich minerals.

In this work, distillers grains-derived hydrochars were prepared by a novel one-pot synthesis through co-HTC with magnesium-rich phyllosilicate clay minerals (vermiculite and attapulgite). It is our central hypothesis that one-pot co-HTC of distillers grains with vermiculite/attapulgite would result in hydrochar with unique surface properties and enhanced ability to sorb various pollutants in water. To test the hypothesis, the physical and chemical properties of grains-derived hydrochars were characterized in detail. In addition, batch sorption experiments were conducted using P and methylene blue (MB, a representative organic cation). Specific objectives are to: 1) determine whether the grains-derived hydrochar can support the clays via co-HTC, 2) understand the mechanism of P and MB adsorption by the composite hydrochar, and 3) identify optimal conditions for P and MB removal by the composite hydrochar.

## 2. Materials and methods

### 2.1. Materials

Distillers grains were obtained from a grain distillery in Guizhou Province, P. R. China. Its basic physical and chemical properties are listed in the Table 1. Vermiculite ($AlFeMgO_3Si$), with a particle size between 0.1 and 0.15 mm, was purchased from Shanghai McLean Biochemical Technology Co., Ltd and attapulgite ($Mg_5Si_8O_{20}(OH)_2(OH_2)_4{\cdot}4H_2O$), with a particle size between 0.1 and 0.15 mm, was purchased from Shanghai Yuanye Biotechnology Co., Ltd. Analytical grade $KH_2PO_4$ and methylene blue (MB) were purchased from Sino Pharm Chemical Reagent Co., Ltd.

### 2.2. Preparation of hydrochar

Prior to co-HTC, attapulgite and vermiculite (5 and 15% by weight, respectively) were separately mixed with distillers grains in a blender. Then, 90 g of each mixture was added to 900 mL (1:10 v/v) ultrapure water for ultrasonic dispersion for 1 h and then placed in a 1500 mL reaction kettle (GSHA, JIAYI, CHINA). A constant voltage was maintained and the temperature was held at 180 ℃ for 6 h, then allowed to cool. After oven-drying, the samples were ground in a mortar and sieved to pass 100 mesh. Samples were stored in a desiccator and designated as DG-A5 (distillers grains −5% attapulgite hydrochar), DG-A15 (distillers grains −15% attapulgite hydrochar), DG-V5 (distillers grains −5% vermiculite hydrochar), and DG-V15 (distillers grains −15% vermiculite hydrochar). Distillers-grains hydrochar was also prepared without the addition of minerals using the same HTC conditions, and labeled as DGH.

### 2.3. Characterization of hydrochar

Scanning electron microscopy (SEM) equipped with energy-dispersive X-ray spectrometry (EDX; JSM-7800F, JEOL, Japan) was used to observe the surface morphology and the proportions of basic elements in the hydrochars. The surface functional groups of hydrochar were analyzed by a Fourier Transform Infrared Spectrometer (FT-IR) (Nicolet 6700, Thermo Fisher Scientific, USA). The crystalline materials and the crystallographic structures of hydrochar were checked through X-ray diffraction (XRD) using an X-ray diffractometer equipped with a graphite crystal monochromator (I-2, Nicolet, Madison, WI, USA). The atomic states of major elements were analyzed by X-ray photoelectron spectroscopy (XPS; Axis Ultra DLD, Kratos, UK) using an Al $K_\alpha$ line (15 kV, 10 mA, 150 W) as a radiation source. In addition, an ICP-MS (Agilent 8800 s, Agilent Technologies, USA) was employed to measure total Mg content. The content of $Mg(OH)_2$ was obtained by titration with chromium-black T and EDTA standard solution (Raij, 1966). Then, according to the ratio coefficient of $Mg(OH)_2$ to MgO, the content of MgO was calculated (Birgitta Bostrom, 1991; Zhu, 2020).

### 2.4. Preliminary adsorption experiments

Initial assessment of the MP and P sorption capacity of the hydrochars was conducted using batch adsorption experiments performed using varying solid:solution ratios. For MB, different amounts of hydrochar (0.01, 0.02, 0.04, 0.1, 0.2, 0.4 g) were added into 50 mL centrifuge tubes with 40 mL of 100 mg $L^{-1}$ MB solution. The centrifuge tube containing the sample was placed in a thermostatic box oscillation shaker set at 160 rpm and 25 ℃ for 12 h. Afterwards, samples were passed through a 0.45 μm nylon membrane filter (Whatman 1004-055, USA) and concentrations of MB in the filtrate were determined by UV spectrophotometry (Ahmad, 2020) with detection at 665 nm wavelength. For P adsorption, 0.01, 0.02, 0.04, 0.08, and 0.1 g of each hydrochar was added to 40 mL of 20 mg $L^{-1}$ P solution. After sorption with the same experimental conditions, concentrations of P in the

**Table 1**
Bulk properties of raw distillers grains.

| sample | pH | Moisture content (wt. %) | Organic matter (wt. %) | C (wt. %) | O (wt. %) | N (wt. %) | Mg (wt. %) | Al (wt. %) |
|---|---|---|---|---|---|---|---|---|
| Distillers grains | 5.97 | 71.8 | 92.2 | 55.5 | 31.3 | 11.3 | 0.1 | 0.1 |

filtrates were determined by UV/Vis spectrophotometry (Murphy and Riley, 1962) with detection at 882 nm wavelength.

Adsorption of each sorbate, Q (mg $g^{-1}$), was calculated as:

$$Q = (C_0 - C_i) \times V/m \quad (1)$$

and the removal efficiency R (%) as:

$$R = (C_0 - C_i)/C_0 \times 100\% \quad (2)$$

where $C_0$ and $C_i$ denote the initial and final sorbate concentrations (mg $L^{-1}$), respectively; $V$ (L) represents the volume of the solution; and $m$ is the mass (g) of the sorbent.

### 2.5. Adsorption kinetics experiments

More detailed examinations of hydrochar adsorption were carried out with 300 mL solutions of 100 mg $L^{-1}$ MB or P with 0.3 g of each hydrochar in 500 mL polyethylene bottles. Using the experimental conditions outlined above, concentrations of MB and P were determined in filtered 10 mL solutions withdrawn after 1, 2, 4, 8, 12, 24, and 48 h (triplicate samples for each time point).

The kinetics data obtained were modeled using pseudo-first order, pseudo-second-order, and Elovich models (Eqs. (3), (4), and (5), respectively):

$$q_t = q_e(1 - exp^{-K_1 t}) \quad (3)$$

$$q_t = K_2 q_e^2 t/(1 + K_2 q_e t) \quad (4)$$

$$q_t = \ln(\alpha\beta t + 1)/\beta \quad (5)$$

where $K_1$ ($h^{-1}$) and $K_2$ (g $mg^{-1}h^{-1}$) are the pseudo-first order and pseudo-second order sorption constants, respectively; $\alpha$ refers to the initial sorption rate; $\beta$ indicates the desorption constant; $q_t$ and $q_e$ (mg $g^{-1}$) are the amount adsorbed at time $t$ and at equilibrium, respectively.

### 2.6. Adsorption isotherm experiments

To construct sorption isotherms, solutions were prepared with initial MB concentrations of 25, 50, 100, 150, 200 mg $L^{-1}$ and initial P concentrations of 15, 30, 45, 60, 90, 120 mg $L^{-1}$. About 0.3 g of each hydrochar sorbent was mixed with 40 mL of MB or phosphate solutions in 50 mL centrifuge tubes for 24 h (triplicate samples for each concentration).

The experimental data was simulated using Langmuir, Freundlich, and Langmuir-Freundlich adsorption models (Eqs. (6), (7), and (8), respectively):

$$q_e = q_{max} K_L C_e/(1 + K_L C_e) \quad (6)$$

$$q_e = K_F C_e^{1/n} \quad (7)$$

$$q_e = q_{max} K_S C_e^n/(1 + K_S C_e^n) \quad (8)$$

where $q_e$ and $C_e$, denote the amount adsorbed (mg $g^{-1}$) and the sorbate concentration (mg $L^{-1}$) at equilibrium, respectively; $K_L$ (L $mg^{-1}$), $K_F$ ((mg $g^{-1}$) (L $mg)^{1/n}$), and $K_S$ (L $mg^{-1}$) represent the Langmuir, Freundlich, and Langmuir-Freundlich adsorption constants, respectively; $q_{max}$ refers to the maximum adsorption capacity; and $n$ is the heterogeneity coefficient.

## 3. Results and discussion

### 3.1. Hydrochar characterization

Studies suggest that the adsorption performance of biochar is closely related to its surface structure (Dos Santos et al., 2019). The unmodified hydrochar had a rough surface, and no apparent pore structure whereas some layered structures appeared on the surface of hydrochars carbonized with minerals (see supplementary material). The hydrochar modified by vermiculite had a larger particle size and a smoother lamellar structure. However, attapulgite-modified hydrochar had less lamellar structure and a few non-uniform pores. These heterogeneous layered clay structures can promote the adsorption of ionic pollutants as suggested by previous studies (Bao et al., 2020; Shen et al., 2020).

Elemental analysis indicated that the low amounts of metal ions in distillers grains were also present in its hydrochar (Table 2). The metal content in hydrochar, such as Mg, Al, and Fe, was increased by its co-carbonization with the clays, which is consistent with the results from the EDX analysis (see supplementary material). The Mg content (and other metals) increased with clay loading; by about 20 times from pristine hydrochar to 5%-clay modified hydrochar for both vermiculite and attapulgite, and by an additional 2 times from 5% to 15%-clay-modified hydrochar for both vermiculite and attapulgite. However, after HTC, a large amount of $Mg(OH)_2$ was found in the modified hydrochars which was not present in the raw clay minerals, likely due to transformation of MgO to $Mg(OH)_2$ at high temperature and pressure during the hydrothermal process. According to the findings of previous studies, both $Mg(OH)_2$ and MgO particles loaded onto biochar have strong P adsorption ability (Yao et al., 2013). This suggests that co-HTC of distillers grains with the two clays may improve the P adsorption of hydrochars.

FT-IR was performed to examine the surface functional groups of the hydrochar samples (see supplementary material). Generally, all hydrochars had a wide strong absorption peak at 3396 $cm^{-1}$ corresponding to the stretching vibration of hydroxyl groups (–OH) and physically sorbed water. Other peaks, such as those at 2923 $cm^{-1}$, 2825 $cm^{-1}$, 1630 $cm^{-1}$, and 1398 $cm^{-1}$ (characteristics of C–H, C = O, and C = C stretching) were also retained after HTC. After the addition of the clays during carbonization, the characteristic peak at about 3396 $cm^{-1}$ was significantly weakened, likely due to the clay minerals inhibiting hydroxylation and improving the stability of biochar, which is consistent with findings of previous research (Fan et al., 2020). With clay addition, absorption peaks appeared at about 1090 $cm^{-1}$ and 467 $cm^{-1}$, which can be attributed to stretching vibration of the Si-O-Si bond and the Si-O bond, respectively (Al. Haddabi et al., 2015). In the composite

**Table 2**
Bulk properties of pristine and distillers grains-derived hydrochars.

| Content | Hydrochar type | | | | |
|---|---|---|---|---|---|
| | DGH | DG-V5 | DG-V15 | DG-A5 | DG-A15 |
| *C* (wt. %) | 72.1 | 60.3 | 55.9 | 67.8 | 63.6 |
| *O* (wt. %) | 25.1 | 29.2 | 33.2 | 26.1 | 27.4 |
| *Mg* (wt. %) | 0.1 | 2.4 | 4.5 | 2.1 | 3.4 |
| *Al* (wt. %) | 0.3 | 1.9 | 2.6 | 0.1 | 0.2 |
| *Si* (wt. %) | 1.1 | 1.9 | 3.8 | 2.8 | 3.9 |
| *P* (wt. %) | 0.1 | 0.1 | 0.1 | 0.2 | 0.2 |
| *Fe* (wt. %) | 0.1 | 0.8 | 1.9 | 0.1 | 0.2 |
| *Mg* (mg $kg^{-1}$) | 597.9 | 11347.3 | 22757.5 | 11785.2 | 22630.3 |
| $Mg(OH)_2$(mg $kg^{-1}$) | 262.0 | 8765.9 | 17219.7 | 8432.5 | 16098.9 |
| *MgO* (mg $kg^{-1}$) | 810.2 | 14347.4 | 25829.5 | 14987.7 | 26393.0 |

hydrochar with attapulgite, C-O also appeared, probably because the original attapulgite contains C-O (Pan et al., 2011). The formation of oxygen-containing functional groups on the surface of clay mineral-loaded hydrochar during the hydrothermal process may improve the ability of hydrochar to adsorb contaminants.

XPS was used to characterize the bonding environments of major elements in pristine and modified hydrochars. As illustrated in (see supplementary material), C 1 s (285.8 eV) and O 1s (533. eV) were found in all the hydrochar samples. The C1s spectrum of DGH (pristine hydrochar) was split into three distinct peaks with binding energies of 284.8, 286.0, and 288.5 eV corresponding to C-C, C-O-C, and C–C = O, respectively. With the addition of clay minerals, C 1s content decreased and O 1s content increased. In addition, two new elements, Fe 2p (713.7 eV) and Mg 1s (1024.3 eV), appeared in the DG-V15% and DG-A15%. The two Mg peaks of DG-V15 correspond to Mg metal (1302.3 ev) and Mg oxide (1304.5 ev); while those of DG-A15 were Mg oxide (1304.5 ev) and $MgCO_3$ (1305.0 ev). The change of elemental ratios in the sample indicates that clay minerals were successfully loaded onto the hydrochar surface after the one-pot co-HTC.

All hydrochars had a distinct XRD peak at 2θ = 26.5° (see supplementary material). After co-HTC with clays, the 26.5° peak became larger, suggesting that co-carbonization with clay enhanced carbonization. Additional peaks at 21.8, 26.4, 36.4, 39.2, 42.2, 45.6, 49.9, 54.6, 59.8, 63.8 and 67.8° 2θ also appeared, which can be attributed to $SiO_2$ in clay minerals, as suggested by previous studies (Al. Haddabi et al., 2015; Mu and Wang, 2015). For DG-V and DG-A, peak 1 (biotite, 2θ = 26.52) and peak 2 (quartz, 2θ = 21.93) were generated in the XRD spectra, suggesting that vermiculite and attapulgite were present in the granular composite (Zhang et al., 2020; Zhu et al., 2020a). After the distillers grains were co-carbonized with vermiculite, the XRD pattern exhibited a crystal structure of $Mg_2C_3$ (XRD peak at 2θ = 34.6°), indicating that C and Mg in vermiculite may react to form crystalline $Mg_2C_3$ through HTC. The crystal structure of $Mg(OH)_2$ appeared clearly in all modified hydrochars, further suggesting the transformation of MgO to $Mg(OH)_2$ during HTC.

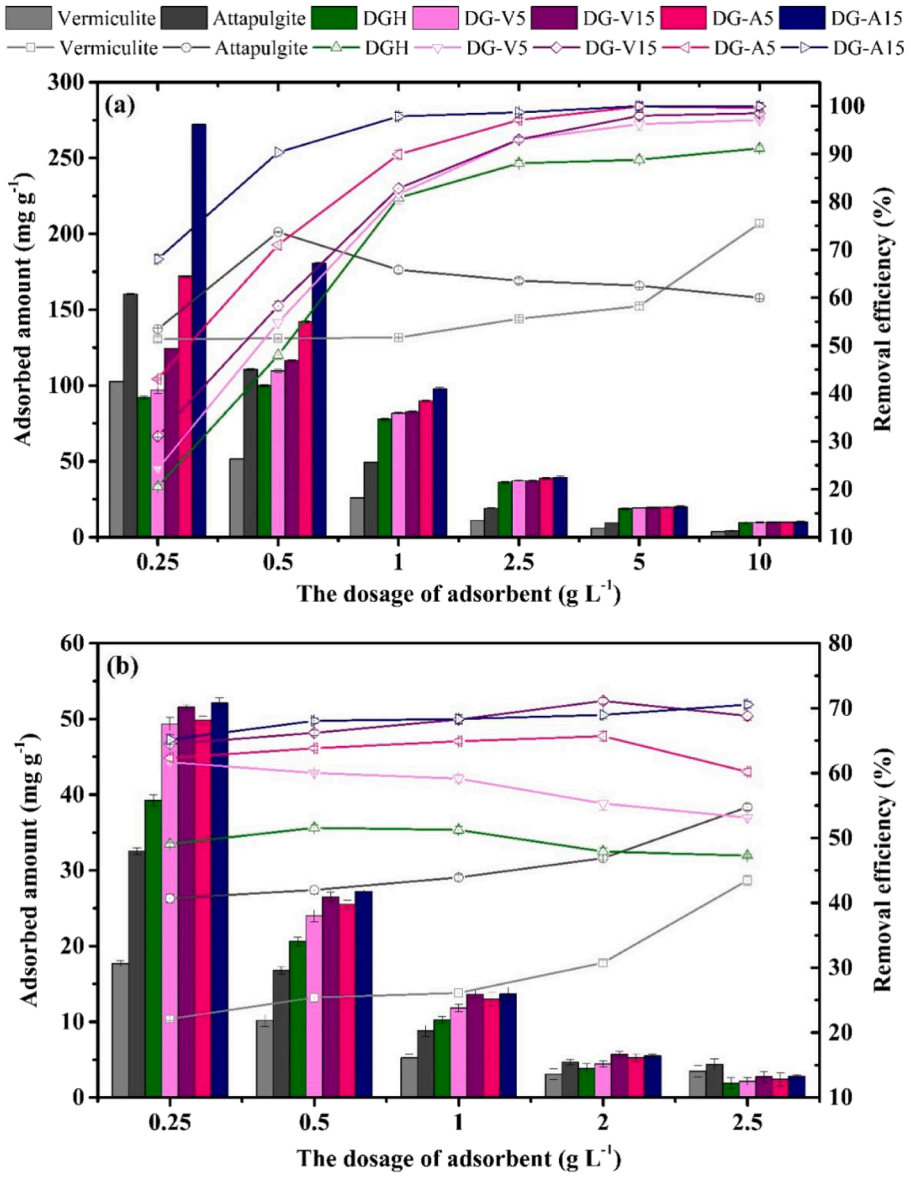


**Fig. 1.** Adsorbed amounts (vertical bars) and removal efficiency (lines) of (a) methylene blue and (b) phosphate from aqueous solution by sorbents of different dosages of distillers grains-derived hydrochars.

### 3.2. Hydrochar adsorption

The removal rate of MB increased rapidly with adsorbent dosage until reaching a maximum sorption capacity of about 272 mg $g^{-1}$ at a dosage of about 0.25 g DG-A15 in 100 mg $L^{-1}$ MB solution (Fig. 1a). For most of the tested dosages, the clay-modified hydrochars showed higher MB removal efficiencies than that of either the pristine hydrochars or the clay minerals alone (Fig. 1a). Sorption of MB by hydrochar modified by vermiculite (as well as hydrochar modified with only 5% attapulgite) was less than or not significantly different from that of the unmodified hydrochar. Thus, the hydrochar modified by attapulgite showed greater MB adsorption (68.0% with a 0.25 g $L^{-1}$ dosage) than that using vermiculite, especially at lower sorbent dosages.

Co-carbonization with both clay types promoted the adsorption of P by distillers grains-derived hydrochar (Fig. 1b), with the maximum removal rates of 71.1% and 70.5% for hydrochar modified with 15% vermiculite and 15% attapulgite, respectively. These two 15% clay modifications increased P adsorption over both the unmodified hydrochar (51.6% maximum) and the 5% clay-loaded forms of these hydrochars (61.6% and 62.3%, respectively). The strong P removal by the two clay minerals was consistent with previous findings (Brigatti et al., 2005; Zhu et al., 2020a). Even though attapulgite showed higher P adsorption than vermiculite, the clay-loaded hydrochars (DG-V15 and DG-A15) had similar P removal efficiencies under the test conditions. This indicates that both clay minerals were equally good modifiers of the distillers grains hydrochar for P removal. According to the XRD results (see supplementary material), HTC changed the MgO in clay minerals into $Mg(OH)_2$ , which would enhance P adsorption by the clay-modified distillers grains hydrochar. Besides, the increase in surface area and the adsorption site likely increased with the increasing adsorbent dosage, leading to greater sorbent removal rate.

Weight-normalized adsorption by DG-A15 was negatively dependent upon the dosage when the solution volume and initial concentration were constant. This suggests that adsorption sites were left vacant on hydrochar and may overlap, reducing the effective contact area and amount of pollutant adsorbed. When the dosage was increased from 0.25 to 1.0 to 10.0 g $L^{-1}$, the adsorption capacity of MB decreased from 272.2 to 97.9 to 10.0 mg $g^{-1}$. Thus, DG-A15 at 1.0 g $L^{-1}$ was selected for optimal MB removal, considering the factors of adsorption capacity, adsorption efficiency, and cost. The removal rate of phosphate did not significantly change with the increasing addition amount. Therefore, DG-A15 at 0.50 g $L^{-1}$ was selected optimal P removal.

### 3.3. Adsorption kinetics

Adsorption of MB onto the attapulgite-modified hydrochars reached equilibrium after about 12 h, after an initial 4 h period in which the MB adsorption rate increased rapidly and then decreased (Fig. 2a). P adsorption to the modified hydrochars occurred more rapidly than MB, reaching equilibrium after about 10 h (Fig. 2b). After the initial fast adsorption period, the hydrochar samples likely slowly removed MB or P through internal diffusive adsorption within the pores after the external surface adsorption sites were saturated (Ahmad, 2020). The MB and P adsorption data were best fitted by the pseudo-second-order model (compared to the pseudo-first-order and Elovich models) (Table 3), suggesting that MB adsorption of distillers grains-derived hydrochar may be controlled by multiple mechanisms (Ding et al., 2016; Fan et al., 2016).

### 3.4. Adsorption isotherms

With regression coefficients > 0.91, the Freundlich model provided a much better fit of MB adsorption isotherm data than the Langmuir model, (Fig. 2c and Table 4), further suggesting that adsorption of MB onto the hydrochars was controlled by multiple mechanisms. The very low the Freundlich linearity parameters (about n = 0.2 for both sorbents) suggests high heterogeneity of binding sites on the adsorbents. Using the Langmuir adsorption model, a maximum MB adsorption capacity of 203.1 and 340.3 mg $g^{-1}$ was calculated for DG-A5 and DG-A15, respectively. These values are comparable or higher than that of many other hydrochar sorbents reported in previous studies (Table S1, supplementary materials).

The adsorption of P by the distillers grains-derived hydrochars was best fitted by the Langmuir-Freundlich isotherm model, although the

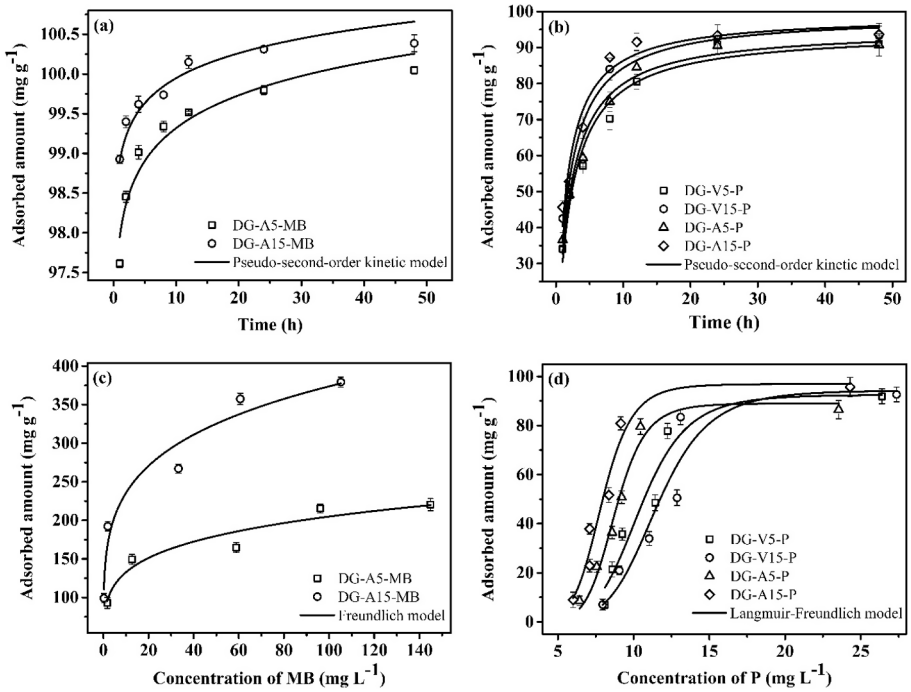


**Fig. 2.** Kinetic of hydrochar sorption of (a) methylene blue and (b) phosphate; and adsorption isotherms for distillers grains-derived hydrochar sorption of (c) methylene blue and (d) phosphate.

**Table 3**
Best-fit model parameter values for adsorption kinetics of MB and P by distillers grains-derived hydrochars.

| Sorbent | Sorbate | Pseudo-first-order kinetic model | | | Pseudo-second-order kinetic model | | | Elovich model | | |
|---|---|---|---|---|---|---|---|---|---|---|
| | | $K_1$ /$h^{-1}$ | $q_e$ / mg·$g^{-1}$ | $R^2$ | $K_2$ /g $mg^{-1}h^{-1}$ | $q_e$ /mg·$g^{-1}$ | $R^2$ | $\alpha$ | $\beta$ | $R^2$ |
| DG-V5 | P | 0.34 | 91.64 | 0.95 | 4.37E-3 | 101.93 | 0.95 | 134.45 | 0.06 | 0.83 |
| DG-V15 | P | 0.29 | 93.07 | 0.95 | 3.69E-3 | 104.01 | 0.94 | 103.63 | 0.05 | 0.83 |
| DG-A5 | P | 0.33 | 91.92 | 0.92 | 4.51E-3 | 101.68 | 0.95 | 152.39 | 0.06 | 0.87 |
| | MB | 4.02 | 99.37 | 0.56 | 4.22E-1 | 99.79 | 0.94 | – | – | – |
| DG-A15 | P | 0.46 | 91.05 | 0.90 | 6.97E-3 | 98.89 | 0.95 | 431.13 | 0.07 | 0.86 |
| | MB | 4.58 | 99.94 | 0.80 | 7.10E-1 | 100.19 | 0.85 | – | – | – |

**Table 4**
Best-fit parameter values for adsorption isotherms of MB and P by distillers grains-derived hydrochars.

| Sorbent | Sorbate | Langmuir adsorption model | | | Freundlich adsorption model | | | Langmuir-Freundlich adsorption model | | | |
|---|---|---|---|---|---|---|---|---|---|---|---|
| | | $K_L$ /L $mg^{-1}$ | $q_{max}$ /mg·$g^{-1}$ | $R^2$ | $K_F$ /(mg $g^{-1}$) (L mg)$^{1/n}$ | n | $R^2$ | $K_S$ /L $mg^{-1}$ | $q_{max}$ /mg·$g^{-1}$ | n | $R^2$ |
| DG-V5 | P | 0.007 | 602.34 | 0.60 | 93.69 | −3.34E4 | 0.91 | 1.31E-7 | 93.34 | 6.75 | 0.92 |
| DG-V15 | P | 0.003 | 1276.82 | 0.58 | 96.39 | −1.24E4 | 0.83 | 5.47E-8 | 94.33 | 6.83 | 0.85 |
| DG-A5 | P | 0.041 | 156.52 | 0.49 | 89.51 | −1.73E5 | 0.93 | 4.79E-9 | 88.98 | 8.82 | 0.97 |
| | MB | 0.373 | 203.05 | 0.74 | 85.97 | 1.89E-1 | 0.92 | – | – | – | – |
| DG-A15 | P | 0.024 | 270.97 | 0.56 | 97.42 | −4.81E4 | 0.92 | 5.97E-8 | 96.91 | 8.05 | 0.93 |
| | MB | 0.863 | 340.28 | 0.79 | 148.39 | 2.01E-1 | 0.95 | – | – | – | – |

Freundlich fits were only slightly lower (Fig. 2d and Table 4). This also indicates that P adsorption on the hydrochar samples were controlled by multiple mechanisms. The average maximum P adsorption capacity was above 89 mg $g^{-1}$ for all the hydrochars tested, but was the greatest for DG-A15 (97 mg $g^{-1}$). These P sorption capacities are also comparable or higher than that of the many other hydrochar sorbents in the literature (see Table S1 Supplementary material).

### 3.5. Adsorption mechanism

The adsorption of pollutants by distillers grains-derived hydrochars is a complex process, and the adsorption mechanism of different pollutants may vary (Fig. 3). The mechanism of adsorption of MB by hydrochars may involve electrostatic attraction, cation exchange, surface complexation, and physical adsorption. FTIR analysis showed that distillers grains-derived hydrochars were rich in diverse functional groups, which can adsorb MB through the electrostatic attraction, cation exchange, and surface complexation mechanisms (Saha et al., 2020). The modified hydrochars showed higher MB adsorption capacities than the pristine hydrochar. This could be attributed to the loading of clay minerals on the hydrochar surface, enhancing the electrostatic attraction, cation exchange, and complexation of MB. XPS results showed that, after adsorbing MB, the C and O contents on the surface of modified hydrochars (DG-V15% and DG-A15%) increased, while the Fe and Mg contents decreased (see supplementary material). This confirms the importance of electrostatic attraction or ion exchange and complexation mechanisms, as some of the Fe and Mg minerals/ions on the sample surface were covered or replaced by MB. The adsorption kinetics and isotherms of the hydrochars to MB were best simulated by the pseudo-second-order kinetic and the Freundlich models, respectively, confirming that the adsorption of MB on the modified hydrochar could be controlled by multiple processes involving electrostatic attraction, ion exchange, complexation, and surface deposition.

Several studies have demonstrated that Mg and Fe minerals on

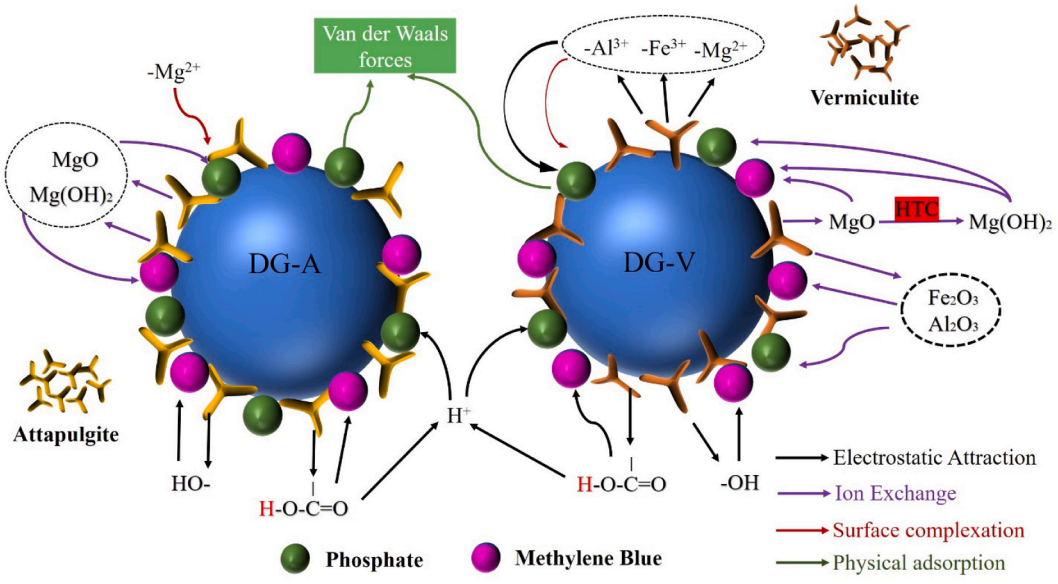


**Fig. 3.** Schematic of proposed distillers grains-derived clay-modified hydrochar sorption mechanisms.

biochar surface are the main adsorption sites for P (De Carvalho Eufrásio Pinto et al., 2019; Yin et al., 2017). In this study, there was also a strong correlation between the clay mineral amounts in hydrochar and the P adsorption amounts. In addition, the XRD spectra of the P-loaded hydrochars (DG-V-P and DG-A-P) showed stronger signals than that of the pristine ones (see supplementary material), suggesting the importance of the loaded clay minerals to P adsorption. In the XPS spectra (see supplementary material) There was no P on the surface of the samples before adsorption. After adsorption, however, P appeared on the sample surface and the XPS characteristic peaks of Fe 2p and Mg 1s shifted, indicating the Mg and Fe minerals on the modified hydrochar surface played important roles in P adsorption. Based on findings of previous studies (Yao et al. 2013; Zheng et al. 2020), adsorption of P on the Mg/Fe minerals on the modified hydrochar surface could be mainly controlled by the electrostatic attraction and surface complexation mechanisms. The modeling results of P adsorption kinetics and isotherms of the hydrochars also confirm the involvement of multiple mechanisms.

### 3.6. Implications

A simple cost-benefit analysis was conducted to determine the feasibility of commercialization of the distillers grains-derived clay-modified hydrochars in China. Table 5 summarizes the components of the analysis. The calculated production cost of clay-modified hydrochar is about 200¥/ton, much lower than the current average market value of commercial hydrochar/biochar (5000¥/ton, Table 5). This result shows the strong techno-economic feasibility of the commercialization of the modified hydrochar from co-HTC of distillers grains and clay minerals. Furthermore, if the modified hydrochars are used to adsorb P from water, the spent hydrochar can be applied as a fertilizer to soils (Yao et al. 2013, Zheng et al. 2019), which would add further economic and environmental benefits in terms of carbon sequestration and nutrient and water retention (Table 5). All these indicate that the novel one-pot production of clay-modified hydrochar from distillers grains is a promising and sustainable technique that is suitable for industrial-scale development in the future. Further investigations thus are needed to promote the commercialization of this technology and to overcome the scale-up challenges such as optimizing the production conditions, reducing operation costs and emissions, and unifying product quality.

## 4. Conclusions

Findings of this study show that one-pot co-HTC of distillers grains with clay minerals produces value-added hydrochar with excellent ability to sorb MB and P in aqueous solution. Among the hydrochar samples, maximum MB and P adsorption capacities of 340.3 and 97.4 mg $g^{-1}$, respectively, was achieved with distillers grains carbonized with 15% attapulgite (DG-A15). Characterization and modeling results suggested that multiple mechanisms controlled the adsorption of MB and P on the hydrochar samples. Cost-benefit analysis revealed the strong economic feasibility of industrial commercialization of clay-modified hydrochar from distillers grains as a sustainable and high efficiency sorbent for environmental applications.

## CRediT authorship contribution statement

**Qingya Xu:** Conceptualization, Methodology, Formal analysis, Investigation, Resources, Data curation, Writing - original draft. **Taoze Liu:** Conceptualization, Validation, Resources, Writing - review & editing, Visualization, Supervision, Project administration, Funding acquisition. **Ling Li:** Investigation, Resources, Writing - review & editing. **Bangyu Liu:** Writing - review & editing. **Xiaodan Wang:** Writing - review & editing. **Shuyi Zhang:** Investigation. **Liangliang Li:** Investigation. **Bing Wang:** Writing - review & editing. **Andrew R. Zimmerman:** Writing - review & editing. **Bin Gao:** Validation, Writing - review & editing.

**Table 5**
Cost-benefit analysisfor commercialization of distillers grains-derived modified hydrochar use (for P versus as a fertilizer) in China.

| Item/operation | Cost/Benefit Parameter | Note |
|---|---|---|
| Industrial HTC reactor capital cost | 30000–40000 ¥ | Including the delivery |
| Reactor life span | 10 years | According to the manufacturer |
| Labor cost per batch | 20–30 ¥ per hour | Salary of a reactor operator |
| Transportation cost per carriage | 200–300 ¥ | Loading and transport of the raw materials by truck |
| Average number of batches a day | 3 | According to the manufacturer |
| Water consumption per batch | 10 ton per ton | Calculated from literature |
| Cost of clay minerals per batch | 2 ¥ $kg^{-1}$ and 50 ¥ $kg^{-1}$ (vermiculite and attapulgite) | Average market price |
| Electric energy consumption | 123 kWh Per ton | According to the manufacturer |
| Tones of $CO_2$ sequestrated | 3 | Based on (Lucian and Fiori, 2017) |
| Hydrochar price | 5000 ¥ $ton^{-1}$ | Average market price of hydrochar |
| Maximum P adsorption capacity | 96.9 mg·$g^{-1}$ | This study |
| Economic benefit of P-loaded hydrochar as a fertilizer | 40 ¥ $ha^{-1}$ | Based on (Yao et al., 2013) |

Note: Costs in yuan (¥)

## Declaration of Competing Interest

The authors declare that they have no known competing financial interests or personal relationships that could have appeared to influence the work reported in this paper.

## Acknowledgments

This work was partially supported by the Natural Science Foundation of China [41930863; U1612441; 41803022].

## Appendix A. Supplementary data

Supplementary data to this article can be found online at https://doi.org/10.1016/j.biortech.2021.125725.

## References

Abd, M.E., El-Hindawy, M.M., Attia, A.I., Mahrose, K.M., 2017. Does the use of distiller's dried grains with solubles (DDGS) in layer diets affect the nutrients digestibility and manure pollution by nitrogen and phosphorous? Environ. Sci. Pollut. Res. Int. 24 (15), 13335–13343.

Ahmad, A.K.N.G., 2020. Removal of methylene blue dye using rice husk, cow dung and sludge biochar: characterization, application, and kinetic studies. Bioresour. Technol. 306, 123202.

Al. Haddabi, M., Vuthaluru, H., Znad, H., Ahmed, M., 2015. Attapulgite as potential adsorbent for dissolved organic carbon from oily water. CLEAN–Soil, Air, Water 43 (11), 1522–1530.

Anh Tuan Vo, V.P.N.A., 2020. Efficient removal of Cr(VI) from water by biochar and activated carbon prepared through hydrothermal carbonization and pyrolysis: adsorption-coupled reduction mechanism. Water-Sui. 11 (6).

Bao, P., Du, H., Xu, X., Li, J., Wu, Y., Zhou, S., Li, L., Lei, N., 2020. Adsorption of Cr (VI) onto attapulgite/UiO-66-$NH_2$ composites from aqueous solution. Integr. Ferroelectr. 209 (1), 125–134.

Birgitta Bostrom, K.B., 1991. Magnesium hydroxide precipitation as pre-enrichment procedure for inductively coupled plasma-atomic emission spectrometric analyses of natural waters 113(2–3), 97–103.

Brigatti, M.F., Colonna, S., Malferrari, D., Medici, L., Poppi, L., 2005. Mercury adsorption by montmorillonite and vermiculite: a combined XRD, TG-MS, and EXAFS study. Appl. Clay Sci. 28 (1-4), 1–8.

De Carvalho Eufrásio Pinto, M., David da Silva, D., Amorim Gomes, A.L., Menezes dos Santos, R.M., Alves de Couto, R.A., Ferreira de Novais, R., Leopoldo Constantino, V. R., Tronto, J., Pinto, F.G., 2019. Biochar from carrot residues chemically modified with magnesium for removing phosphorus from aqueous solution. J. Clean. Prod. 222, 36–46.

Ding, G., Wang, B., Chen, L., Zhao, S., 2016. Simultaneous adsorption of methyl red and methylene blue onto biochar and an equilibrium modeling at high concentration. Chemosphere 163, 283–289.

Dos Santos, K.J.L., Dos Santos, G.E.d.S., De Sá, Í.M.G.L., Ide, A.H., Duarte, J.L.d.S., de Carvalho, S.H.V., Soletti, J.I., Meili, L., 2019. Wodyetia bifurcata biochar for methylene blue removal from aqueous matrix. Bioresour. Technol. 293, 122093.

Fan, E., Hu, F., Miao, W., Xu, H., Shao, G., Liu, W., Li, M., Wang, H., Lu, H., Zhang, R., 2020. Preparation of g-$C_3N_4$/vermiculite composite with improved visible light photocatalytic activity. Appl. Clay Sci. 197, 105789.

Fan, S., Tang, J., Wang, Y., Li, H., Zhang, H., Tang, J., Wang, Z., Li, X., 2016. Biochar prepared from co-pyrolysis of municipal sewage sludge and tea waste for the adsorption of methylene blue from aqueous solutions: kinetics, isotherm, thermodynamic and mechanism. J. Mol. Liq. 220, 432–441.

Fang, J., Gao, B., Chen, J., Zimmerman, A.R., 2015. Hydrochars derived from plant biomass under various conditions: characterization and potential applications and impacts. Chem. Eng. J. 267, 253–259.

Fang, J., Zhan, L., Ok, Y.S., Gao, B., 2018. Minireview of potential applications of hydrochar derived from hydrothermal carbonization of biomass. J. Ind. Eng. Chem. 57, 15–21.

Kumar, J.W.G.V., 2020. Recent trends in biochar production methods and its application as a soil health conditioner: a review. SN Appl. Sci. 2, 1307.

Li, B., Guo, J., Lv, K., Fan, J., 2019. Adsorption of methylene blue and Cd(II) onto maleylated modified hydrochar from water. Environ. Pollut. 254, 113014.

Li, F., Zimmerman, A.R., Hu, X., Yu, Z., Huang, J., Gao, B., 2020. One-pot synthesis and characterization of engineered hydrochar by hydrothermal carbonization of biomass with $ZnCl_2$. Chemosphere 254, 126866.

Lucian, M., Fiori, L., 2017. Hydrothermal carbonization of waste biomass: process design, modeling, energy efficiency and cost analysis. Energies 10 (2), 211.

Miliotti, E., Casini, D., Rosi, L., Lotti, G., Rizzo, A.M., Chiaramonti, D., 2020. Lab-scale pyrolysis and hydrothermal carbonization of biomass digestate: characterization of solid products and compliance with biochar standards. Biomass Bioenerg. 139, 105593.

Mu, B., Wang, A., 2015. One-pot fabrication of multifunctional superparamagnetic attapulgite/ $Fe_3O_4$/ polyaniline nanocomposites served as an adsorbent and catalyst support. J. Mater. Chem. A 3 (1), 281–289.

Murphy, J., Riley, J.P., 1962. A modified single solution method for the determination of phosphate in natural waters - ScienceDirect. Anal. Chim. Acta 27, 31–36.

Padilla-Ortega, E., Medellín-Castillo, N., Robledo-Cabrera, A., 2020. Comparative study of the effect of structural arrangement of clays in the thermal activation: evaluation of their adsorption capacity to remove Cd(II). J. Environ. Chem. Eng. 8 (4), 103850.

Pan, J., Xu, L., Dai, J., Li, X., Hang, H., Huo, P., Li, C., Yan, Y., 2011. Magnetic molecularly imprinted polymers based on attapulgite/$Fe_3O_4$ particles for the selective recognition of 2,4-dichlorophenol. Chem. Eng. J. 174 (1), 68–75.

Quintelas, C., Figueiredo, H., Tavares, T., 2011. The effect of clay treatment on remediation of diethylketone contaminated wastewater: uptake, equilibrium and kinetic studies. J. Hazard. Mater. 186 (2-3), 1241–1248.

Raij, B.V., 1966. Determinação de cálcio e magnésio pelo EDTA em extratos ácidos de solos Calcium and magnesium determination in soils with EDTA. Bragantia 25 (2), 317–326.

Román, S., Ledesma, B., Álvarez, A., Coronella, C., Qaramaleki, S.V., 2020. Suitability of hydrothermal carbonization to convert water hyacinth to added-value products. Renew. Energ. 146, 1649–1658.

Sadeghi, S.H., Hazbavi, Z., Harchegani, M.K., 2016. Controllability of runoff and soil loss from small plots treated by vinasse-produced biochar. Sci. Total Environ. 541, 483–490.

Saha, N., Volpe, M., Fiori, L., Volpe, R., Messineo, A., Reza, M.T., 2020. Cationic dye adsorption on hydrochars of winery and citrus juice industries residues: performance, mechanism, and thermodynamics. Energies 13 (18), 4686.

Shen, T., Wang, L., Zhao, Q., Guo, S., Gao, M., 2020. Single and simultaneous adsorption of basic dyes by novel organo-vermiculite: a combined experimental and theoretical study. Colloids Surf., A 601, 125059.

Vinoth Kumar Ponnusamya, B.S.N.R., 2020. Review on sustainable production of biochar through hydrothermal liquefaction: physico-chemical properties and applications. Bioresour. Technol. 310, 123414.

Wang, B., Lian, G., Lee, X., Gao, B., Li, L., Liu, T., Zhang, X., Zheng, Y., 2020. Phosphogypsum as a novel modifier for distillers grains biochar removal of phosphate from water. Chemosphere 238, 124684.

Wang, S., Gao, B., Zimmerman, A.R., Li, Y., Ma, L., Harris, W.G., Migliaccio, K.W., 2015. Removal of arsenic by magnetic biochar prepared from pinewood and natural hematite. Bioresour. Technol. 175, 391–395.

Yao, Y., Gao, B., Fang, J., Zhang, M., Chen, H., 2014. Characterization and environmental applications of clay-biochar composites. Chem. Eng. J. 242, 136–143.

Yao, Y., Gao, B., Chen, J., Yang, L., 2013. Engineered biochar reclaiming phosphate from aqueous solutions: mechanisms and potential application as a slow-release fertilizer. Environ. Sci. Technol. 47 (15), 8700–8708.

Yin, Q., Zhang, B., Wang, R., Zhao, Z., 2017. Biochar as an adsorbent for inorganic nitrogen and phosphorus removal from water: a review. Environ. Sci. Pollut. R. 24 (34), 26297–26309.

Zhang, D., Xu, Y., Li, X., Wang, L., He, X., Ma, Y., Zou, D., 2020. The immobilization effect of natural mineral materials on Cr(VI) remediation in water and soil. Int. J. Env. Res. Pub. He. 17 (8), 2832.

Zhang, H., Xue, G., Chen, H., Li, X., 2018. Magnetic biochar catalyst derived from biological sludge and ferric sludge using hydrothermal carbonization: preparation, characterization and its circulation in Fenton process for dyeing wastewater treatment. Chemosphere 191, 64–71.

Zheng, Y., Wang, B., Wester, A.E., Chen, J., He, F., Chen, H., Gao, B., 2019. Reclaiming phosphorus from secondary treated municipal wastewater with engineered biochar. Chem. Eng. J. 362, 460–468.

Zheng, Y., Zimmerman, A.R., Gao, B., 2020. Comparative investigation of characteristics and phosphate removal by engineered biochars with different loadings of magnesium, aluminum, or iron. Sci. Total Environ. 747, 141277.

Zhu, D., Chen, Y., Yang, H., Wang, S., Wang, X., Zhang, S., Chen, H., 2020a. Synthesis and characterization of magnesium oxide nanoparticle-containing biochar composites for efficient phosphorus removal from aqueous solution. Chemosphere 247, 125847.

Zhu, S., Wang, S., Yang, X., Tufail, S., Chen, C., Wang, X., Shang, J., 2020b. Green sustainable and highly efficient hematite nanoparticles modified biochar-clay granular composite for Cr(VI) removal and related mechanism. J. Clean. Prod. 276, 123009.

Zhu, Y., 2020. Determination of rare earth elements in seawater samples by inductively coupled plasma tandem quadrupole mass spectrometry after coprecipitation with magnesium hydroxide. Talanta 209, 120536.